

# SEARCH FOR THE PROCESS $e^+e^- \rightarrow \eta'(958)$ WITH THE CMD-3 DETECTOR

R.R.Akhmetshin<sup>a,b</sup>, A.V.Anisenkov<sup>a,b</sup>, V.M.Aulchenko<sup>a,b</sup>,  
 V.Sh.Banzarov<sup>a</sup>, N.S.Bashtovoy<sup>a</sup>, D.E.Berkaev<sup>a,b</sup>, A.E.Bondar<sup>a,b</sup>,  
 A.V.Bragin<sup>a</sup>, S.I.Eidelman<sup>a,b</sup>, D.A.Epifanov<sup>a,e</sup>, L.B.Epshteyn<sup>a,c</sup>,  
 A.L.Erofeev<sup>a</sup>, G.V.Fedotov<sup>a,b</sup>, S.E.Gayazov<sup>a,b</sup>,  
 A.A.Grebenuk<sup>a,b</sup>, D.N.Grigoriev<sup>a,b,c</sup>, E.N.Gromov<sup>a</sup>,  
 F.V.Ignatov<sup>a,b</sup>, S.V.Karpov<sup>a</sup>, V.F.Kazanin<sup>a,b</sup>, **B.I.Khazin**<sup>a,b</sup>,  
 I.A.Koop<sup>a,b</sup>, O.A.Kovalenko<sup>a,b</sup>, A.N.Kozyrev<sup>a</sup>, E.A.Kozyrev<sup>a,b</sup>,  
 P.P.Krokovny<sup>a,b</sup>, A.E.Kuzmenko<sup>a,b</sup>, A.S.Kuzmin<sup>a,b</sup>,  
 I.B.Logashenko<sup>a,b</sup>, P.A.Lukin<sup>a,b</sup>, K.Yu.Mikhailov<sup>a</sup>,  
 N.Yu.Muchnoi<sup>a,b</sup>, V.S.Okhapkin<sup>a</sup>, Yu.N.Pestov<sup>a</sup>,  
 E.A.Perevedentsev<sup>a,b</sup>, A.S.Popov<sup>a,b</sup>, G.P.Razuvaev<sup>a,b</sup>,  
 Yu.A.Rogovsky<sup>a</sup>, A.L.Romanov<sup>a</sup>, A.A.Ruban<sup>a</sup>, N.M.Ryskulov<sup>a</sup>,  
 A.E.Ryzhenenkov<sup>a,b</sup>, V.E.Shebalin<sup>a,b</sup>, D.N.Shemyakin<sup>a,b</sup>,  
 B.A.Shwartz<sup>a,b</sup>, D.B.Shwartz<sup>a,b</sup>, A.L.Sibidanov<sup>a,d</sup>,  
 P.Yu.Shatunov<sup>a</sup>, Yu.M.Shatunov<sup>a</sup>, E.P.Solodov<sup>a,b,1</sup>, V.M.Titov<sup>a</sup>,  
 A.A.Talyshev<sup>a,b</sup>, A.I.Vorobiov<sup>a</sup>, Yu.V.Yudin<sup>a,b</sup>

<sup>a</sup>*Budker Institute of Nuclear Physics, SB RAS, Novosibirsk, 630090, Russia*

<sup>b</sup>*Novosibirsk State University, Novosibirsk, 630090, Russia*

<sup>c</sup>*Novosibirsk State Technical University, Novosibirsk, 630092, Russia*

<sup>d</sup>*University of Sydney, School of Physics, Falkiner High Energy Physics,  
 NSW 2006, Sydney, Australia*

<sup>e</sup>*University of Tokyo, Department of Physics, 7-3-1 Hongo Bunkyo-ku  
 Tokyo, 113-0033, Japan*

---

## Abstract

A search for the process  $e^+e^- \rightarrow \eta'(958)$  in the  $\pi^+\pi^-\eta \rightarrow \pi^+\pi^-\gamma\gamma$  final state has been performed with the CMD-3 detector at the VEPP-2000  $e^+e^-$  collider. Using an integrated luminosity of  $2.69 \text{ pb}^{-1}$  collected at the center-

---

<sup>1</sup>Corresponding author: solodov@inp.nsk.su

of-mass energy  $E_{\text{c.m.}} = 957.68$  MeV we set an upper limit for the product of electronic width and branching fractions  $\Gamma_{\eta'(958) \rightarrow e^+e^-} \cdot \mathcal{B}_{\eta'(958) \rightarrow \pi^+\pi^- \eta} \cdot \mathcal{B}_{\eta \rightarrow \gamma\gamma} < 0.00041$  eV at 90% C.L.

---

## 1. Introduction

Direct production of C-even resonances in  $e^+e^-$  collisions is possible via a two-photon intermediate state. A search for direct production of the  $\eta'(958)$ ,  $f_0(980)$ ,  $a_0(980)$ ,  $f_2(1270)$ ,  $f_0(1300)$ , and  $a_2(1320)$  was performed with the ND detector at the VEPP-2M collider [1]. Only upper limits have been set, in particular, for the electronic width of the  $\eta'(958)$  a limit  $\Gamma_{\eta'(958) \rightarrow e^+e^-} < 0.06$  eV at 90% C.L. has been obtained. In the unitarity limit, when both photons are assumed to be real, the branching fraction of the decay of the  $\eta'(958)$ , denoted below as  $\eta'$ , to an  $e^+e^-$  pair,  $\mathcal{B}_{\eta' \rightarrow e^+e^-}$ , can be estimated using the two-photon branching fraction  $\mathcal{B}_{\eta' \rightarrow \gamma\gamma} = 0.0220 \pm 0.0008$  [2] and the expression from Refs. [3, 4]

$$\mathcal{B}_{\eta' \rightarrow e^+e^-} = \mathcal{B}_{\eta' \rightarrow \gamma\gamma} \frac{\alpha^2}{2\beta} \left( \frac{m_e}{m_{\eta'}} \right)^2 \left[ \ln \left( \frac{1+\beta}{1-\beta} \right) \right]^2 = (3.75 \pm 0.14) \times 10^{-11}, \quad (1)$$

where  $\alpha$  is the fine structure constant,  $m_e$  and  $m_{\eta'}$  are masses of electron and  $\eta'$ , respectively, and  $\beta = \sqrt{1 - 4\left(\frac{m_e}{m_{\eta'}}\right)^2}$ . Using a total width of the  $\eta'$ ,  $\Gamma_{\eta'} = 0.198 \pm 0.009$  MeV [2], we obtain in the unitarity limit  $\Gamma_{\eta' \rightarrow e^+e^-} = (7.43 \pm 0.29) \times 10^{-6}$  eV. Photon virtuality and the  $\eta' \rightarrow \gamma\gamma$  transition form factor can significantly enhance, by a factor of 5-10, the electronic width value, as discussed in Ref. [4].

An observation of the direct production of C-even resonances in  $e^+e^-$  collisions, and, in particular, of the reaction  $e^+e^- \rightarrow \eta'(958)$ , could help to develop theoretical approaches to a photon-loop calculation, which is a crucial point in the estimation of the hadronic light-by-light contribution [5, 6] to the muon anomalous magnetic moment (g-2) [7].

In this paper we report a search for the process  $e^+e^- \rightarrow \eta'(958)$  in the  $\eta'(958) \rightarrow \pi^+\pi^- \eta \rightarrow \pi^+\pi^- \gamma\gamma$  decay chain. The search is based on the  $2.69 \text{ pb}^{-1}$  of an integrated luminosity collected with the CMD-3 detector at the

center-of-mass (c.m.) energy of the VEPP-2000 collider [8, 9] close to the nominal  $\eta'(958)$  mass:  $m_{\eta'} = 957.78 \pm 0.06 \text{ MeV}/c^2$  [2].

## 2. Detector and data taking conditions

The total width of the  $\eta'$  is relatively small, and it is very important to have c.m. energy close to this value. The collider beam energy was continuously monitored during the whole period of data taking (12 days) using the Back-Scattering-Laser-Light system [10]. Figure 1 shows measurements of the beam energy,  $E_{\text{beam}}$ , which demonstrate relatively good stability of the collider energy. The average value of the c.m. energy is  $E_{\text{c.m.}}^{\text{av.}} = 957.678 \pm 0.014 \text{ MeV}$  with a few deviations of up to 0.2 MeV, corresponding to less than 5% of the integrated luminosity, which are still within an energy spread of the collider beams as shown below.

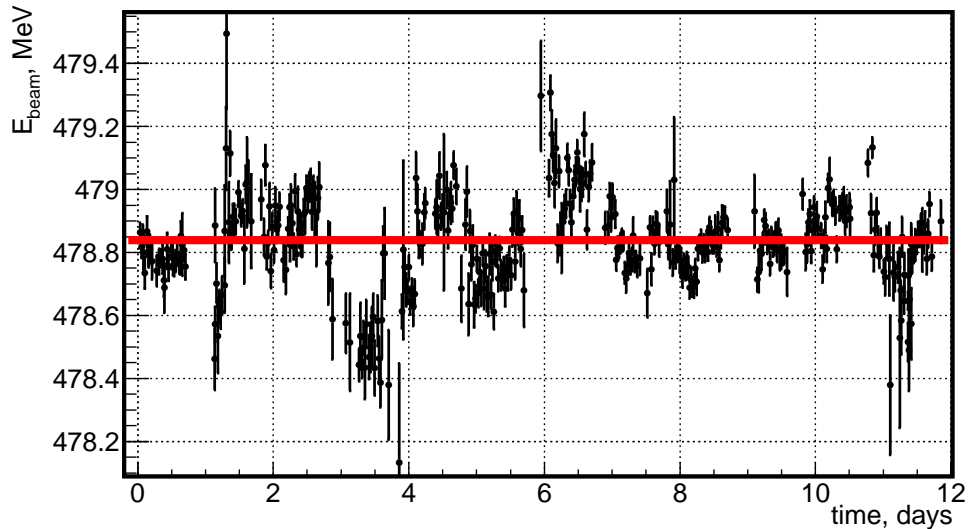


Figure 1: Beam energy measurements during data taking.

The beams of the collider have an energy spread mainly due to the quantum effects of the synchrotron radiation. The c.m. energy spread of the VEPP-2000 collider  $\sigma_{E_{\text{c.m.}}} = 0.246 \pm 0.030 \text{ MeV}$  is calculated according to

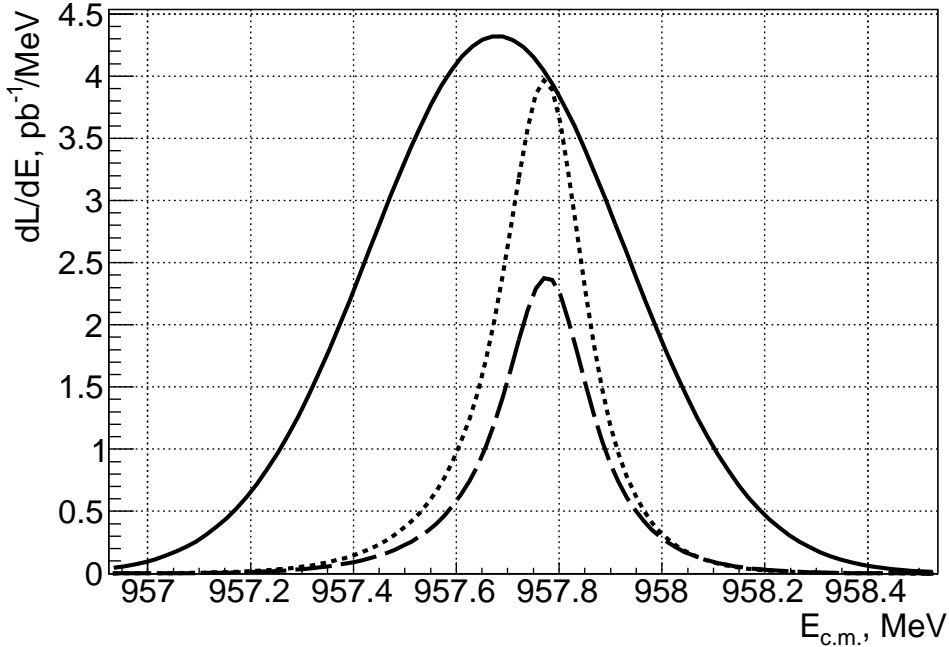


Figure 2: The luminosity distribution versus the c.m. energy (solid line) with an area normalized to the  $2.69 \text{ pb}^{-1}$  of integrated luminosity. The areas below the dotted and dashed lines illustrate an “effective” luminosity for the  $\eta'$  BW and BW convolved with the radiator function, respectively.

Ref. [11] using a longitudinal distribution of the interaction region  $\sigma_z = 2.3$  cm and RF cavity voltage  $V_{\text{cav}} = 18$  kV. Full energy spread (FWHM = 0.590 MeV) is significantly larger than the width of  $\eta'$ , as demonstrated in Fig. 2. A solid line in Fig. 2 shows a differential luminosity distribution  $dL/dE$  versus the c.m. collision energy, with an area normalized to the total integrated luminosity  $L = 2.69 \text{ pb}^{-1}$ . This distribution should be convolved with a Breit-Wigner (BW) function, describing the  $\eta'$  line shape (the dotted line in Fig. 2). Radiation of photons by initial particles changes a collision energy and the BW should be additionally convolved with a radiator function described in Ref. [12, 13]. These radiative corrections decrease the number of signal events by approximately 40%. The area under the dashed line in Fig. 2 illustrates the “effective” integrated luminosity for  $\eta'$  production in

our experiment in comparison with the total integrated luminosity under the solid line.

If we describe the  $\eta'$  production cross section as

$$\sigma^f(E) = \frac{\sigma_{\eta' \rightarrow f}^0 m_{\eta'}^2 \Gamma_{\eta'}^2}{(m_{\eta'}^2 - E^2)^2 + E^2 \Gamma_{\eta'}^2}, \quad (2)$$

where  $\sigma_{\eta' \rightarrow f}^0$  is the peak cross section for the process  $e^+e^- \rightarrow \eta'$  with  $\eta'$  decay to the final state  $f$ , we can calculate an integrated production cross section as

$$\sigma_{\text{int}}^f = \int_0^{E_{\text{beam}}} dE \int_0^1 \frac{1}{\sqrt{2\pi}\sigma_{\text{E.c.m.}}} e^{-\frac{(\text{E.c.m.}^{\text{av.}} - E)^2}{2\sigma_{\text{E.c.m.}}^2}} \cdot F(x, E) \cdot \sigma^f(E(1-x)) dx, \quad (3)$$

where  $F(x, E)$  is the radiator function [12, 13], and  $x$  is a fraction of energy taken by photons. Using a relation

$$\sigma_{\eta' \rightarrow f}^0 \Gamma_{\eta'} = 4\pi \frac{C \cdot \mathcal{B}_{\eta' \rightarrow f} \cdot \Gamma_{\eta' \rightarrow e^+e^-}}{m_{\eta'}^2}, \quad (4)$$

where  $\mathcal{B}_{\eta' \rightarrow f}$  is the branching fraction to the measured final state  $f$ , and  $C = 3.89 \cdot 10^{11}$  nb MeV<sup>2</sup> is a conversion constant [2], we perform the integration of Eq. 3, and obtain  $\sigma_{\text{int}}^f = (6.38 \pm 0.23) \cdot \Gamma_{\eta' \rightarrow e^+e^-}$  (eV)  $\cdot \mathcal{B}_{\eta' \rightarrow f}$  nb for our experimental conditions. The error in the coefficient reflects uncertainty in the  $\sigma_{\text{E.c.m.}}$  value due to variation of cavity voltage  $V_{\text{cav}}$ , and uncertainty in the beam energy ( $\text{E.c.m.}^{\text{av.}}$ ) measurements, including energy instability according to Fig. 1, weighted with the fraction of integrated luminosity during the energy shifts. Since the energy spread is significantly larger than the total  $\eta'$  width, the integrated cross section is proportional to the product of the  $\eta'$  electronic width and branching fraction to the measured final state  $f$ , calculated as

$$\Gamma_{\eta' \rightarrow e^+e^-} \cdot \mathcal{B}_{\eta' \rightarrow f} = \frac{N}{6.38 \cdot \epsilon^f \cdot L} \text{ (eV)}, \quad (5)$$

where  $N$  is the number of observed signal events and  $\epsilon^f$  is a detection efficiency for the final state  $f$ .

For the studied decay mode with  $\mathcal{B}_{\eta' \rightarrow \pi^+\pi^-} = 0.429$  [2], the calculated cross section for the unitarity limit of  $\Gamma_{\eta' \rightarrow e^+e^-}$  is very small,  $\sigma_{\text{int}} \approx$

$2 \times 10^{-5}$  nb, and should be compared with the cross section of the single-photon reaction  $e^+e^- \rightarrow \pi^+\pi^-\eta$ . The events of this process were observed only above  $E_{\text{c.m.}} > 1200$  MeV and the energy dependence of the cross section was well described in the model where the final state is produced via three interfering resonances –  $\rho(770)$ ,  $\rho(1450)$  and  $\rho(1700)$ , see for example Ref. [19]. At  $E_{\text{c.m.}} = 958$  MeV we obtain  $\sigma_{e^+e^- \rightarrow \pi^+\pi^-\eta} = (1.2 \pm 0.6) \times 10^{-3}$  nb with large uncertainty from the unknown interference phases between the  $\rho$  resonances extrapolating to the region close to the threshold. This value is comparable or larger than the two-photon cross section  $\sigma_{\text{int}}$  with possible enhancement due to the form factor, and to prove signal observation a measurement outside  $\eta'(958)$  mass is needed. Note that the  $\eta' \rightarrow \pi^0\pi^0\eta$  decay mode is free from the single-photon physical background, and we plan to use it for such a study as well.

The general-purpose detector CMD-3 has been described in detail elsewhere [14]. Its tracking system consists of a cylindrical drift chamber (DC) [15] and double-layer multiwire proportional Z-chamber, both also used for a trigger, and both inside a thin ( $0.2 X_0$ ) superconducting solenoid with a field of 1.3 T. The liquid xenon (LXe) barrel calorimeter with  $5.4 X_0$  thickness has fine electrode structure, providing 1-2 mm spatial resolution [16], and shares the cryostat vacuum volume with the superconducting solenoid. The barrel CsI crystal calorimeter [16] with a thickness of  $8.1 X_0$  is placed outside the LXe calorimeter, and the end-cap BGO calorimeter with a thickness of  $13.4 X_0$  is placed inside the solenoid [17]. The luminosity is measured using events of Bhabha scattering at large angles [18].

### 3. Selection of $e^+e^- \rightarrow \pi^+\pi^-\gamma\gamma$ events

Candidates for the process under study are required to have two good charged-particle tracks and two or more clusters in the calorimeters not related to tracks assumed to be photons. We use the following “good” track definition:

- A track contains more than five hits in the DC.

- A track momentum is larger than 40 MeV/c.
- A minimum distance from a track to the beam axis in the transverse plane is less than 0.5 cm.
- A minimum distance from a track to the center of the interaction region along the beam axis Z is less than 10 cm.
- A track has a polar angle large enough to cross half of the DC radius.

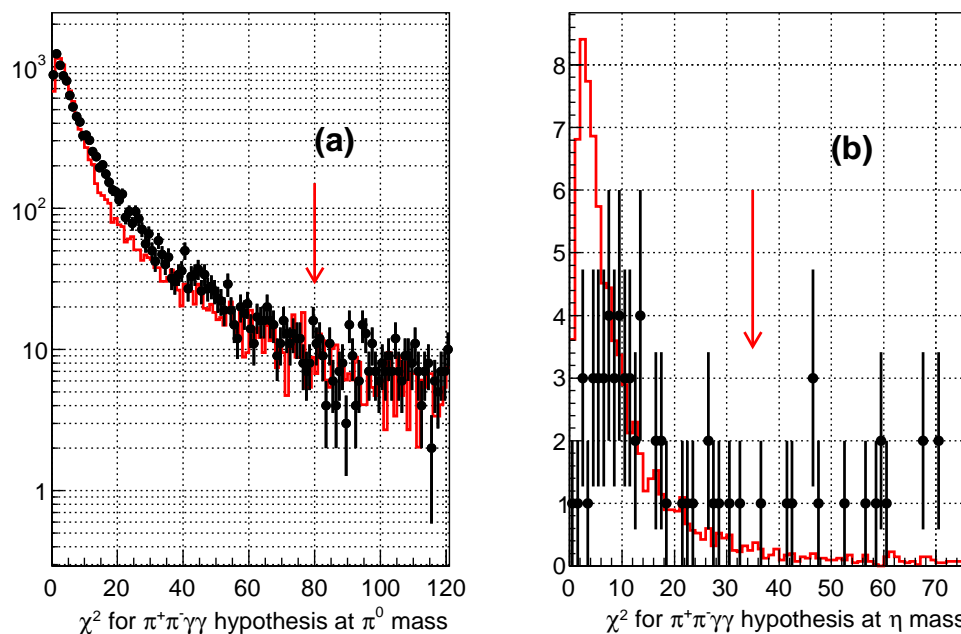


Figure 3: The  $\chi^2$  distribution of events with two tracks and two photons for the  $e^+e^- \rightarrow \pi^+\pi^-\gamma\gamma$  hypothesis for data (dots) and corresponding simulations (histograms), when the two-photon invariant mass is in the  $\pm 35$  MeV/ $c^2$  window around the  $\pi^0$  mass (a) and in the  $\pm 35$  MeV/ $c^2$  window around the  $\eta$  mass (b).

Two tracks are required to have opposite charges and are assumed to be pions. The detected photons are required to have more than 25 MeV energy deposition in the calorimeters. Reconstructed momenta and angles of the detected charged tracks and energy and angles of two photons are subject to

the kinematic fit, assuming that the total energy is equal to  $E_{\text{c.m.}}$  and total momentum is equal to zero. The covariance matrices for charged tracks and photons are used in the fit and provide a  $\chi^2$  value for each event. If an event candidate has more than two photons, the photon pair with the smallest  $\chi^2$  value is retained. As a result of the fit, we obtain improved values of the momenta, energies and angles for all particles. The main contribution to the selected sample comes from the process  $e^+e^- \rightarrow \pi^+\pi^- \pi^0 \rightarrow \pi^+\pi^- \gamma\gamma$ . We perform simulation of the processes  $e^+e^- \rightarrow \pi^+\pi^- \pi^0$  and  $e^+e^- \rightarrow \eta'$  and apply all experimental conditions and selections to the simulated samples. We use the  $e^+e^- \rightarrow \pi^+\pi^- \pi^0$  events to verify our simulation. Figure 3(a) shows the  $\chi^2$  distributions for the experimental (dots) and simulated  $e^+e^- \rightarrow \pi^+\pi^- \pi^0$  (histogram) events when the invariant mass of the photon pair is in the  $\pm 35 \text{ MeV}/c^2$  window around the  $\pi^0$  mass. A vertical arrow shows the applied selection. Figure 3(b) presents the  $\chi^2$  distributions for the event candidates, in which the invariant mass of the photon pair is in the  $\pm 35 \text{ MeV}/c^2$  window around the  $\eta$  mass for data (points), and the simulated distribution for the process  $e^+e^- \rightarrow \eta' \rightarrow \pi^+\pi^- \eta \rightarrow \pi^+\pi^- \gamma\gamma$  (histogram). The  $\chi^2$  distributions for data and simulation for the  $\pi^0$  signal in Fig. 3(a) are in good agreement, and tighter selection shown by the vertical arrow in Fig. 3(b) changes the number of  $\pi^+\pi^- \pi^0$  signal events by 1% only. After this selection some candidate events for the process  $e^+e^- \rightarrow \eta'$  are observed.

Figure 4(a) shows a scatter plot of the total energy deposition in the calorimeter,  $E_{\text{total}}$ , versus two-photon invariant mass for selected experimental  $\pi^+\pi^- \gamma\gamma$  events. A clear signal of the  $\pi^+\pi^- \pi^0$  events is seen. Simulated events for the processes  $e^+e^- \rightarrow \pi^+\pi^- \pi^0 \rightarrow \pi^+\pi^- \gamma\gamma$  and  $e^+e^- \rightarrow \eta' \rightarrow \pi^+\pi^- \eta \rightarrow \pi^+\pi^- \gamma\gamma$  are shown in Fig. 4(b). The experimental sample contains a relatively large number of background events from various quantum electrodynamics processes, when scattered electron and positron are accompanied with a number of radiative photons. These processes leave significant amount of energy in the calorimeter and can be effectively suppressed by requiring  $E_{\text{total}} < 0.7 \cdot E_{\text{c.m.}}$  (solid lines in Fig. 4), retaining 87%



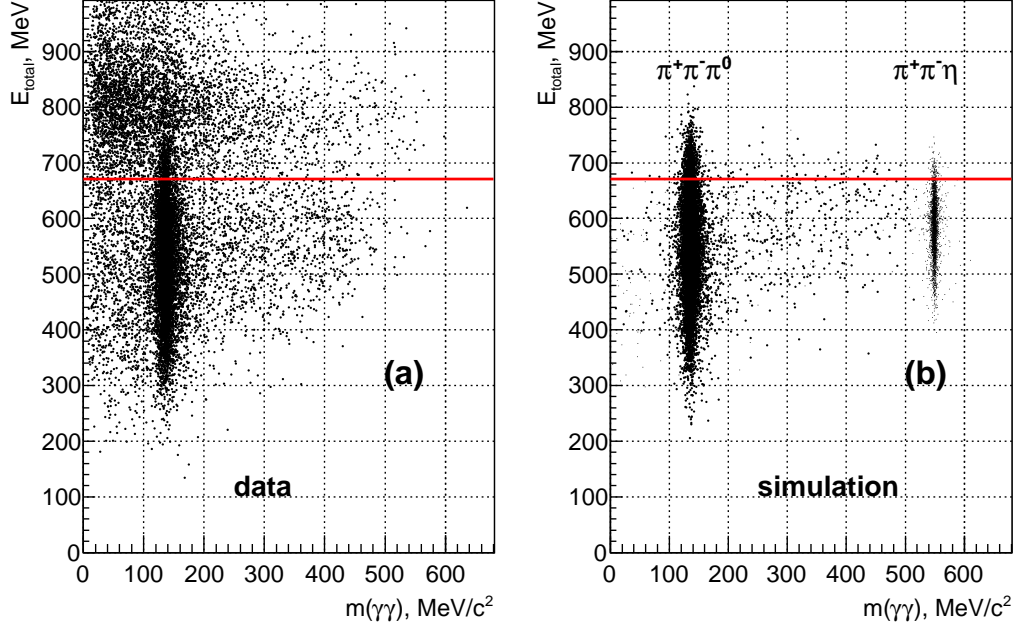


Figure 4: Scatter plot of the total energy deposition versus two-photon invariant mass for selected experimental  $\pi^+\pi^-\gamma\gamma$  events (a) and simulated  $\pi^+\pi^-\pi^0 \rightarrow \pi^+\pi^-\gamma\gamma$  and  $\eta' \rightarrow \pi^+\pi^-\eta \rightarrow \pi^+\pi^-\gamma\gamma$  events (b). Solid lines show applied selection.

of signal events in good agreement with simulation.

We calculate the detection efficiency from the  $e^+e^- \rightarrow \pi^+\pi^-\eta \rightarrow \pi^+\pi^-\gamma\gamma$  simulated events as a ratio of the number of events after selections described above to the total number of generated events and obtain  $\epsilon^f = 31.1\%$  for this final state.

Using the signal from the process  $e^+e^- \rightarrow \pi^+\pi^-\pi^0 \rightarrow \pi^+\pi^-\gamma\gamma$ , and taking into account 1% data-simulation corrections for charged tracks and 2% for the photons, we found that overall data-simulation discrepancy gives less than 5% uncertainty in the resulting efficiency for applied selections.

Figure 5 shows a projection plot of Fig. 4(a) after the applied selections. Dots are for data, and the histogram shows the invariant mass of two photons from the simulated process  $e^+e^- \rightarrow \pi^+\pi^-\pi^0 \rightarrow \pi^+\pi^-\gamma\gamma$ . The expanded view of the 450-650  $\text{MeV}/c^2$  region is shown in the box with the shape of

signal for the process  $e^+e^- \rightarrow \eta' \rightarrow \pi^+\pi^- \eta \rightarrow \pi^+\pi^- \gamma\gamma$  (histogram) obtained from the simulation. The line shows the expected level of background, obtained from the fit of events in this region with a second-order polynomial function. We found no event candidates for this process in the signal region, and estimate the expected background of  $1.0 \pm 0.5$  events. We use a conservative estimate of the number of signal events as  $N < 2.0$  at 90% C.L. using the Feldman-Cousins approach [20], assuming no observed events and expected background of 0.5 events.

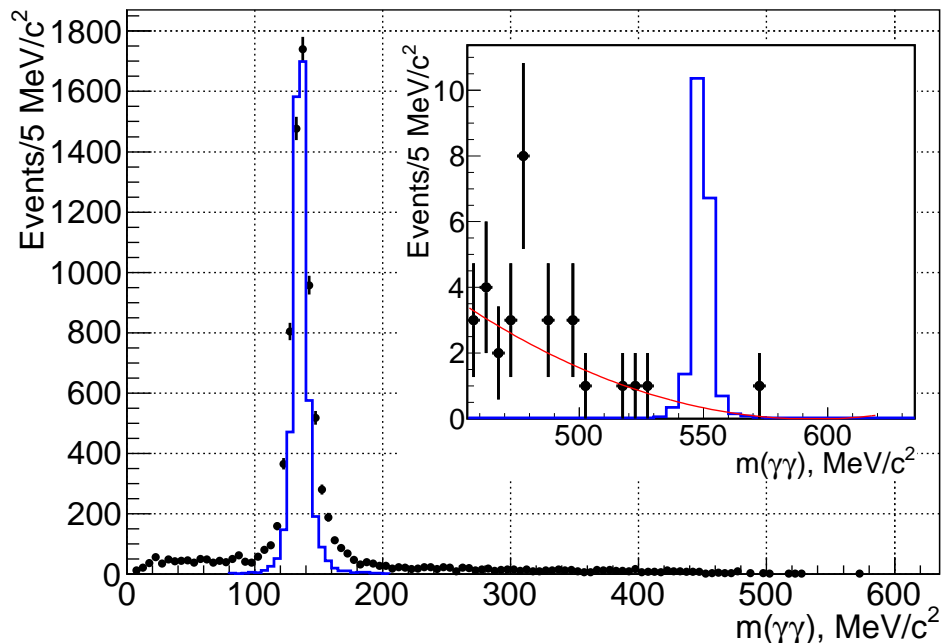


Figure 5: Projection plot of Fig. 4 after the applied cut on total energy. Dots are from data, the histogram shows invariant mass of two photons from the simulated process  $e^+e^- \rightarrow \pi^+\pi^- \pi^0 \rightarrow \pi^+\pi^- \gamma\gamma$ . The expanded view of the 450-650  $\text{MeV}/c^2$  region is shown in the box with the signal shape of the process  $e^+e^- \rightarrow \eta' \rightarrow \pi^+\pi^- \eta \rightarrow \pi^+\pi^- \gamma\gamma$  (histogram) expected from simulation, and expected level of background (line).

Using Eq. 5 we obtain the result

$$\Gamma_{\eta' \rightarrow e^+e^-} \mathcal{B}_{\eta' \rightarrow \pi^+\pi^-} \mathcal{B}_{\eta \rightarrow \gamma\gamma} < \frac{2.0}{6.38 \cdot 0.311 \cdot 2690} = 0.00037 \text{ eV at 90\% C.L..}$$

After taking into account the systematic uncertainties on luminosity (2%), efficiency (5%), and beam energy instability (5%) we conservatively increase the upper limit by 12%:

$$\Gamma_{\eta' \rightarrow e^+e^-} \mathcal{B}_{\eta' \rightarrow \pi^+\pi^-} \mathcal{B}_{\eta \rightarrow \gamma\gamma} < 0.00041 \text{ eV at 90\% C.L..}$$

The decay rates of  $\eta' \rightarrow \pi^+\pi^- \eta$  and  $\eta \rightarrow \gamma\gamma$  are relatively well known, and using the values from Ref. [2] we obtain  $\Gamma_{\eta' \rightarrow e^+e^-} < 0.0024 \text{ eV}$  at 90% C.L.. Finally, from the total width of the  $\eta'$  from Ref. [2] we calculate  $\mathcal{B}_{\eta' \rightarrow e^+e^-} < 1.2 \times 10^{-8}$ , that should be compared to the value from the ND experiment [1],  $\mathcal{B}_{\eta' \rightarrow e^+e^-} < 2.1 \times 10^{-7}$  listed in the PDG tables [2]. The latter value was obtained from the limit  $\Gamma_{\eta' \rightarrow e^+e^-} < 0.06 \text{ eV}$  and  $\eta'$  width of about 300 keV known at that time.

In our experiment we can also set a limit on the cross section for the process  $e^+e^- \rightarrow \pi^+\pi^- \eta$  at  $E_{\text{c.m.}} = 957.7 \text{ MeV}$ , which is found to be  $\sigma(e^+e^- \rightarrow \pi^+\pi^- \eta) = N/(\epsilon_{\pi^+\pi^- \eta} L) < 6.1 \text{ pb}$  for 90 C.L., where  $\epsilon_{\pi^+\pi^- \eta} = \epsilon^f \cdot \mathcal{B}_{\eta \rightarrow \gamma\gamma} = 0.122$  is a detection efficiency for this process.

## Conclusion

We search for direct production of the C-even  $\eta'(958)$  meson in  $e^+e^-$  collisions. A special experimental run of the VEPP-2000 collider was performed at the c.m. energy close to the  $\eta'$  mass with a  $2.69 \text{ pb}^{-1}$  integrated luminosity. We found no event candidates for the process  $e^+e^- \rightarrow \eta'(958) \rightarrow \pi^+\pi^- \eta \rightarrow \pi^+\pi^- \gamma\gamma$  and obtain the upper limit for the product  $\Gamma_{\eta'(958) \rightarrow e^+e^-} \mathcal{B}_{\eta' \rightarrow \pi^+\pi^-} \mathcal{B}_{\eta \rightarrow \gamma\gamma} < 0.00041 \text{ eV}$ . This limit is ten times lower compared to the previous measurement [1].

## Acknowledgements

The authors are grateful to A. Kupś for stimulating discussions and to M. N. Achasov for help with energy calibration. We thank the VEPP-2000 personnel for the excellent machine operation.

This work is supported in part by the Russian Education and Science Ministry (grant N 14.610.21.0002, identification number RFMEFI61014X0002),

by the Russian Foundation for Basic Research grants RFBR 13-02-00991-a, RFBR 13-02-00215-a, RFBR 12-02-01032-a, RFBR 13-02-01134-a, RFBR 14-02-00580-a, RFBR 14-02-31275-mol-a, RFBR 14-02-00047-a, RFBR 14-02-31478-mol-a, RFBR 14-02-91332 and the DFG grant HA 1457/9-1.

## REFERENCES

- [1] P. Vorobev *et al.* (ND Collaboration) Sov. J. Nucl. Phys. **48**, 273 (1988).
- [2] J. Beringer *et al.* (Particle Data Group), Phys. Rev. D **86**, 1 (2012) and 2013 partial update for the 2014 edition.
- [3] S. D. Drell, Nuovo Cim. **11**, 693 (1959).
- [4] L. G. Landsberg, Phys. Rep. **128**, 301 (1985).
- [5] J. Prades, E. de Rafael, A. Vainshtein, arXiv:0901.0306.
- [6] G. Colangelo *et al.*, JHEP 1409, 091 (2014), G. Colangelo *et al.*, Phys. Lett. B **738**, 6 (2014).
- [7] M. Davier, S. Eidelman, A. Höcker, Z. Zhang, Eur. Phys. J. C**31**, 503 (2003).
- [8] V.V. Danilov *et al.*, Proceedings EPAC96, Barcelona, p.1593 (1996).
- [9] I.A.Koop, Nucl. Phys. B (Proc. Suppl.) **181-182**, 371 (2008).
- [10] V. Abakumova *et al.*, Phys. Rev. Lett. **110**, 140402 (2013).
- [11] I. Koop, private communication. The c.m. energy spread  $\sigma_{E_{c.m.}}$  (keV) for VEPP-2000 is related to the RF cavity voltage  $V_{cav}$  (kV), beam energy  $E_{beam}$  (GeV), and longitudinal collision length  $\sigma_Z$  (mm) as

$$\sigma_{E_{c.m.}} = 4.05 \cdot \sigma_Z \cdot \sqrt{V_{cav} \cdot E_{beam} \cdot \sin(\arccos(63.2E_{beam}^4/V_{cav}))}.$$

- [12] E.A. Kuraev and V.S. Fadin, Sov. J. Nucl. Phys. **41**, 466 (1985).
- [13] S. Actis *et al.*, Eur. Phys. J. C**66**, 585 (2010).
- [14] B.I.Khazin, Nucl. Phys. B (Proc. Suppl.) **181-182**, 376 (2008).
- [15] F. Grancagnolo *et al.*, Nucl. Instr. Meth. A**623**, 114 (2010).
- [16] A.V.Anisyonkov *et al.*, Nucl. Instr. Meth. A**732**, 463 (2013).
- [17] D. Epifanov (CMD-3 Collaboration), J. Phys. Conf. Ser. **293**, 012009 (2011).

- [18] R.R. Akhmetshin *et al.* (CMD-3 Collaboration), Nucl. Phys. B (Proc. Suppl.) **225-227**, 69 (2012).
- [19] V. Cherepanov and S. Eidelman, Nucl. Phys. Proc. Suppl. **218**, 231 (2011).
- [20] G. J. Feldman and R. D. Cousins, Phys. Rev. D **57**, 3873 (1998).